INTERNATIONAL JOURNAL OF AUTOMOTIVE AND MECHANICAL ENGINEERING
ISSN: 2229-8649 e-ISSN: 2180-1606
VOL. 21, ISSUE 2, 2024, 11426 – 11437
DOI: https://doi.org/10.15282/ijame.21.2.2024.19.0882

RESEARCH ARTICLE

Influence of Friction Stir Processing on the Hardness and Tribological Properties of Aluminium-Magnesium Alloys

Vinay Papanna[1,2]* and Basava Kumar K G[3]

[1]Faculty of Mechanical Engineering, PES University, Bengaluru, 560100 Karnataka, India
[2]Visvesvaraya Technological University, Belagavi, 590018 Karnataka, India
[3]Global Campus, Visvesvaraya Technological University, Belagavi, 590018 Karnataka, India

ABSTRACT - In this study, we have employed friction stir processing to strategically modify the microstructure of AA-Mg alloys, resulting in a direct enhancement of their mechanical properties. The experiments encompassed a range of tool speeds ranging from 800 to 1600 rpm and feed rates ranging from 20 to 80 mm/min. Employing a single-pass approach across all combinations, samples were extracted from the stir zone region to evaluate hardness and wear characteristics. The evaluation involved Vickers hardness tests to quantify hardness and pin-on-disc tests to examine the tribological attributes of the specimens. The worn-out surfaces of the specimens were examined using scanning electron microscope imagery. There is a substantial increase in hardness when compared with the base material, i.e., 78 HVN is up to 96 HVN for 20 mm/min at 1200 rpm, 98 HVN for 20 mm/min at 800 rpm, 106 HVN for 60 mm/min at 1600 rpm and 96 HVN for 80 mm/min at 1600 rpm. Furthermore, the coefficient of friction increased from 0.341 for base materials to a maximum of 0.635, 0.667, 0.604, and 0.646 for the same combination of speed and feed rate, respectively. The maximum change in percentage is 26% in hardness and 49% in wear coefficient.

ARTICLE HISTORY
Received : 18th Aug 2023
Revised : 09th Feb 2024
Accepted : 07th June 2024
Published : 20th June 2024

KEYWORDS
Friction Stir Processing
Aluminium alloys
Hardness
Wear
Microstructure

1.0 INTRODUCTION

Friction stir processing, an innovative surface treatment technique derived from friction stir welding, offers a distinct advantage by addressing casting defects and effecting refined and uniform grain structures in secondary nonferrous alloys [1, 2]. This process employs a non-consumable tool featuring a shoulder and pin, as illustrated in Figure 1. The lower surface of the shoulder contacts the material, generating heat through friction, while the pin stirs the softened metal to perform the actual work. Originally designed for softer materials, this method has also been successfully extended to harder materials like cast iron and titanium steel [2].

Within the friction stir zone, three distinct regions are discerned: the nugget region, the thermo-mechanically affected zone, and the heat-affected zone [1, 2]. The nugget zone experiences high temperatures and plastic deformation, directly influencing fine and uniaxial grain deformation. In the thermo-mechanically affected zone, characterized by medium temperatures and deformation, recrystallized grains are prevalent. The heat-affected zone primarily experiences temperature variations and precipitation. Compared to fusion welding, friction stir welding imparts superior strength, fatigue resistance, and ductility [2].

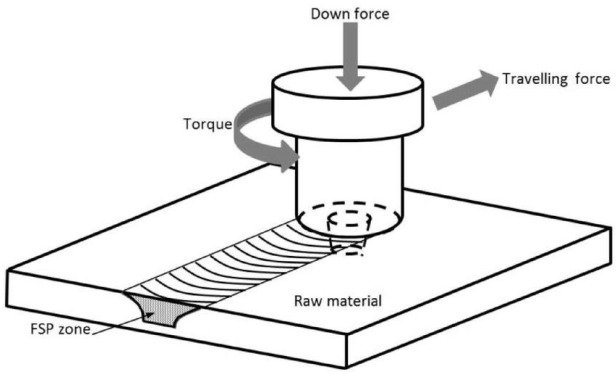

Figure 1. Schematic diagram of friction-stir processing

Friction stir processing offers a novel method for producing hybrid composites that integrate diverse secondary alloys by single and multiple passes. The mechanical properties were measured and increased in multiple passes to induce fine-grained structures and even particle distribution [3]. Specifically, the hybrid composite exhibited a remarkable 34% increase in hardness, 14% in ultimate strength, and a substantial 42% decrease in wear rate [4]. FSP was used to fabricate

*CORRESPONDING AUTHOR | Vinay Papanna | ✉ vinaypapanna@gmail.com

Al-Cr-O hybrid nanocomposites and obtained a homogenous distribution of secondary particles near the nugget region, and wear properties were dominated after FSP [5]. The tool's rotational speed and transverse feed significantly influence its mechanical properties. [6]. It is important that the friction-stir process is used to develop the secondary alloys in terms of refined, homogeneous, and uniformly distributed structures, which enhance the mechanical properties [4, 5, 6].

The grain size and hardness near the stir zone were observed after friction stir processing of 5005-H34 and 7075-T651 with different pin profiles. Mechanical properties are more influenced by transverse feed than rotational speed. The distribution of particles near the stir zone was reduced when the speed increased [7]. FSP is used to eliminate the porosity in the interlayer, which is formed due to the additive manufacturing of 4043 aluminum alloy. After the FSP process, the mechanical properties and microstructure were observed and validated with the material without FSP. The average yield and ultimate were 88 and 148 MPa, respectively. The fatigue strength and elongation increased by 28% and 108.7%, respectively. The material after FSP will have high ductility and fatigue performance [28]. The pin in the tool is not only to generate heat through friction and plastic deformation by localized material movement around the pin. A concurrent flow of material from the front to the back of the pin, filling the tool wake's void, contributes to changes in grain characteristics, orientation, and the elimination of casting defects. These transformations exert a direct influence on the hardness and mechanical attributes of the base metal [8].

For sound welding or processing, more attention to the tool geometry and process parameters is essential. For hardened materials such as steel, cast iron, and titanium alloys, tool wear is also an important parameter but can be neglected for soft materials. Investigating the influence of the process parameters on properties such as hardness, tensile strength, impact resistance, and elongation in the friction stir processing [9]. The Taguchi method was used to find the percentage of contribution, such as rotational speed, transverse speed, and tilt angle, which are 48.56%, 43.52%, and 5.78%, respectively [10]. In the present work, only two parameters, i.e., speed and feed, are varied in the study of the properties. Impact of tool speeds on microstructure and mechanical attributes on Ti-6Al-4V joints, and the optimal range is between 400 and 600 rpm, coupled with a feed rate of 75 mm/min [11]. Tool shoulder diameters between 18 to 24 mm will produce defect-free zones in 6 mm thick plates of AZ31B magnesium alloy for different process parameter combinations [12]. Tool durability, both square and triangular pin profiles, are evaluated, with longer pin lengths leading to wider interference zones and heightened tensile properties [13, 14]. The Stationary shoulder friction stir process was done on the AA7075-T651 aluminum alloy by varying the rotational speed from 600 to 1000 rpm, and other parameters were kept constant. Due to the SSFSP unfirm grain refinement and reduction in grain size up to 2-3 μm from 15 μm. The elongation increased up to 50% by reducing 10 % in ultimate tensile strength. The rotational speed of the tool tip will have minimal influence on properties, but the shoulder speed will increase grain refinement and increase ductile properties [29]. The tool ratio of shoulder diameter to pin diameter (D/d) was varied on LM25AA-5%SiCp metal matrix composites, the ratio of 3 is optimum [15]. Threaded taper pins yield the most uniformly distributed particles within the stir zone, manifesting complete onion ring patterns [7, 15]. The hardness increased from 83 HV to 162 HV in the AA6360 alloy, from 85 HV to 295 HV in the 6082 alloy, and from 107 HV to 155 HV in the AA6061 alloy after friction stir processing [19]. The AA2285 alloy showed an increase in hardness with higher rotational speeds [20]. In the case of AA-17% Si, an increase in welding speed led to elevated microhardness as well as improved ultimate properties and elongation percentages [21]. The influence of process parameters on properties after FSP was studied. In the present work, the rotational speed varies from 680 to 900 rpm, and the feed rate and plug depth are kept constant throughout the experiment. The hardness was measured near the weld region, and tensile tests were done. When compared with base metal, both properties were increased due to the temperature effects of grain refinement, which made the material ductile [24]. Comparing the tool-affected zones with the base metal, both the retreating and advancing sides displayed increased hardness. The hardness increased near the stir zone for feed rates of 120 and 160 mm/min across all speeds and decreased for the feed rate of 80 mm/min for the ASM356 alloy after friction stir processing [22]. For the LM28 AA-Si alloy, friction stir processing resulted in increased hardness and improved tensile properties due to porosity elimination and a uniform distribution of Si particles. Hardness increased by up to 32%, accompanied by reductions in mean area size and aspect ratio [23]. The Tool parameter was varied with rotational and dwell time to join the dissimilar materials by using FSW. The length of the pin was varied, and its mechanical properties were studied. Three conical pins of three lengths were used in the experiment, and the short-length pin was able to increase the microhardness at the top surface compared with the other two. The longer the length, the harder the lower surface. The length will positively affect the properties, and tool rotational speed will be a second influence factor in the process [25]. Magnesium was able to be incorporated into the aluminum by using FSP at a percentage of 2, 4.5, and 33.9. Hardness was increased from 25 to 208.4 HV, and due to the presence of magnesium, corrosion resistance was increased, which will match the requirement for marine applications [26]. The Laser deposition method will produce porosity in the samples. FSP was used to overcome the porosity in the material. The presence of porosity and grain size was measured before and after FSP. Due to the FSP, secondary grains were distributed evenly in the base material, which reduced the porosity from 1.4% to 0.04%. The grain size was reduced by 86% when compared to the deposited zone [30]. Due to their beneficial properties, aluminum and its alloys find widespread application across diverse domains. However, conventional cast alloys often exhibit inadequate strength for critical applications, necessitating secondary modification methods like friction stir processing, heat treatment, coating, etc. The advantages of aluminum-magnesium alloys, such as strain hardening, moderate strength, corrosion resistance, and toughness, render them invaluable in applications spanning construction, infrastructure, storage vessels, and more [16].

While researchers have explored the optimization of process parameters for optimizing mechanical properties, it remains incomplete. In the area of friction stir processing, investigations into mechanical properties within the aluminium-magnesium series (5-series) are notably absent. Prior efforts largely focus on hardness and tensile attributes, neglecting tribological properties. This study seeks to bridge this gap by examining shifts in hardness and tribological behaviors and establishing a linkage between these characteristics.

2.0 EXPERIMENTAL WORK

The present experimental investigation focuses on utilizing AA-Mg alloys as the base material, produced through die casting, with the specific composition outlined in Table 1. Initial cast blocks measuring 185 x 155 x 15 mm are subjected to machining to achieve precise dimensions suitable for the tool holding mechanism within the friction stir processing machine. Characterization of hardness and chemical composition is conducted on the base material. A non-consumable tool, engineered from H13 tool steel, exhibits a hardness range of 58-62 HRC. The tool is equipped with a threaded, straight-profiled pin, with detailed dimensions illustrated in Figure 2.

Table 1. The composition of Aluminium-alloy (Base material) in weight %

Element	Weight percentage
Mg	1.91 to 2.18
Al	Balancing
Other Alloys (Fe, Si, Mn, Cu, etc.)	< 0.5
Yield Strength	395 - 406 MPa
Tensile Strength	465 - 477 MPa
Elongation	8.8 to 9.2 %

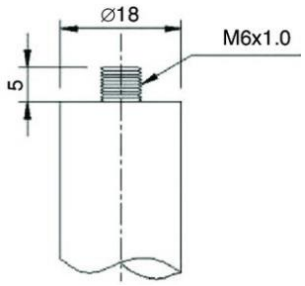

Figure 2. Tool used in the present work, dimensions in mm

After the preparation of plates and tools, the plates are affixed to a work-holding device, interfacing with a dynamometer to measure forces. The friction stir process is executed utilizing a 4-axis, 25-ton capacity machine manufactured by BISS India. Detailed machine process parameters are enumerated in Table 2. Notably, the experimentation encompasses three sample plates, each undergoing four passes wherein the speed remains constant while feed rates vary. For instance, sample 1 employs a speed of 800 rpm and feed rates of 20, 40, 60, and 80 mm/min. Similar arrangements are established for samples 2 and 3 at speeds of 1200 and 1600 rpm, respectively, with the same feed rates and executed in ascending order of feed rates from 20 to 80 mm/min, as depicted in Figure 3.

Table 2. Process parameters in the experiment work [10]

Tool speed (rpm)	Feed rate (mm/min)	Tilt angle (deg)	Tool material	Pin profile
800, 1200 and 1600	20, 40, 60 and 80	0^0	H13 Steel	Threaded and straight

(i) (ii)

Figure 3. Friction stir process on sample for different speeds (i) 800 rpm, (ii) 1200 rpm

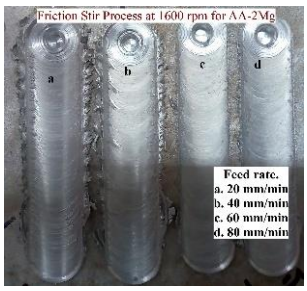

(iii)

Figure 3. (cont.) (iii) 1600 rpm

For wear and hardness testing, specimens are shaped through wire EDM, as illustrated in Figure 4. The evaluation commences with Vickers hardness testing, where a pyramid-shaped indenter with an apical angle of 136° is employed, following ASTM E384 standards. The unit of the hardness given by the test is Vicker's Pyramid Number (HV). Testing adheres to a load of 15 Kgf and a dwell time of 15 seconds [17]. Hardness is gauged across the advancing and retreating sides of the tool, perpendicular to the friction stir process path. Notably, the highest hardness is observed within the nugget zone, followed by diminishing values in the thermo-mechanical and heat-affected zones. While fluctuations in hardness are noticeable on the top and middle surfaces, the bottom region retains the base material's hardness. For the investigation of tribological properties, pin-on-disc tests are conducted as per ASTM G99-04 standards [18]. Samples are acquired from the stir zone with an 8 mm pin diameter. The tests employ a 3 kg load, a 15-minute duration, and a sliding distance of 1650 m. The counterpart disc is crafted from E24 steel with a hardness of 58 HRC and a roughness of 0.2 μm. Prior to testing, both specimens and discs undergo a cleaning process. Test specimens are mounted on a specially designed holder, facilitating contact with the rotating disc. The interaction generates coefficient of friction data, stored digitally for later analysis.

$$\text{Wear Rate } (\text{mm}^3/\text{N.m}) = \frac{\text{Volume loss in mm}^3}{\text{Sliding distance x Applied laod (N.m)}} \quad (1)$$

The calculation of volumetric loss entails measuring the mass of each specimen using a milligram-precision weighing scale before and after testing. Wear loss calculations are derived from pertinent equations. Throughout the testing, coefficients of friction are systematically recorded against time for varying combinations of speed and feed rate. In the interest of comparative analysis, both the base material and friction-stir-processed specimens are subjected to hardness and wear tests. The friction stir process contributes to strain hardening in the nugget region, yet this is accompanied by increased brittleness due to the presence of magnesium alloys. Upon completion of wear tests, scanning electron microscopy is employed to examine the worn surfaces at different magnifications, specifically 40 μm and 100 μm intensities. Surface textures are meticulously scrutinized and correlated with the established coefficients of friction.

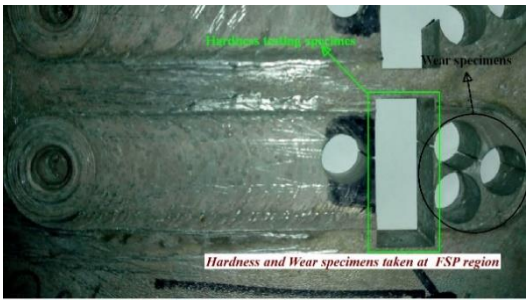

(a)

(b)

(c)

Figure 4. Friction stir process surface samples (a) cut section in FSP region, (b) hardness sample and (c) wear test sample

4.0 RESULTS AND DISCUSSION

After the completion of the friction stir processing, the specimens are meticulously prepared for the two primary experimental analyses: hardness testing and wear testing. Comprehensive tests were carried out for every tool rotational speed and feed rate pairing. In a parallel manner, the base material underwent testing under identical conditions, enabling a systematic comparison of the property alterations resulting from surface modification when juxtaposed with the unprocessed base material. Below, the ensuing sections delve into the test results, graphical representations, and ensuing discussions:

4.1 Microhardness Test

In the current study, one reading was taken at the center of the friction stir region, while five readings were obtained on both sides of the tool. An average of two readings was calculated for each trial, and the resulting data was plotted in terms of average values as shown in Figure 5 (a), (b), (c), and (d). The processed surface's hardness varies with changes in rotational speed and speed rate. Both of these parameters play a role in altering hardness and mechanical properties, and their manipulation is a focal point of the current study. Among the collected data, the highest hardness recorded is 106 VHN, achieved at a speed of 1600 rpm with a feed rate of 60 mm/min. Compared with the original material, the maximum recorded increase in hardness is 26%, while the minimum is 13%. The distribution of hardness changes is not consistent. When the material is in a softer state and subjected to the thrust load, it contracts and densifies compared to the base material. High rotational speed coupled with a low feed rate generates enough heat to soften the material, but if the tool engages too late, heat dissipation occurs. Intriguingly, hardness alterations exhibit an increasing trend across trials, even with the lowest rotational speed and highest feed rate. Rotational speed significantly impacts material heating. Lower feed rates result in minimal heat loss and primarily induce strain hardening. Similarly, when the speed is low, but the feed rate is high, hardness increases due to strain-hardening effects. Magnesium was able to be in the aluminum by using FSP at a percentage of 2, 4.5, and 33.9. Hardness was increased from 25 to 208.4 HV, and due to the presence of magnesium, corrosion resistance was increased, which will match the requirement for marine applications [26].

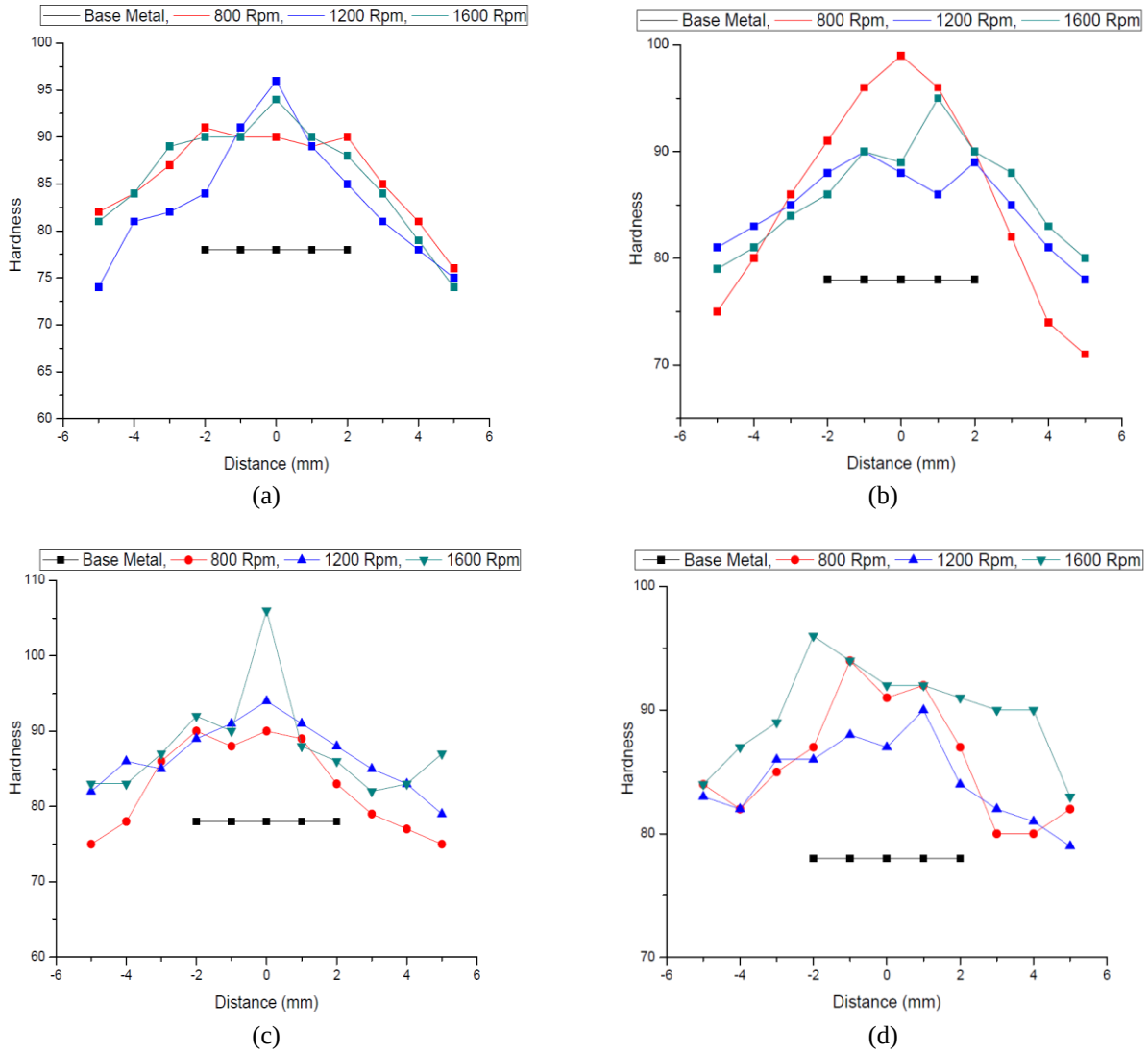

Figure 5. Microhardness (HVN) of FSP surface for different feed rates (a) 20 mm/min, (b) 40 mm/min, (c) 60 mm/min and (d) 80 mm/min

The experimental setup featured a pin diameter of 6 mm, with the inner and outer diameters of the shoulder surface measuring 6 mm and 18 mm, respectively. Five readings were taken within the pin region, while three readings were collected on both sides of the shoulder surface. The resulting data was represented graphically, with the nugget region between -2 and +2 and the remaining zones between -2 and -5 and +2 and +5 on both sides of the tool. The graphs illustrated the average harnesses, allowing for comparison with the base material. In each case, the speed remained constant while the feed rate was varied, specifically at 20 mm/min, 40 mm/min, 60 mm/min, and 80 mm/min. The most substantial hardness change occurred at a feed rate of 40 mm/min and a rotational speed of 800 rpm. Notable variations in hardness were also observed at combinations such as a feed rate of 20 and 60 mm/min with a speed of 800 rpm and a feed rate of 40 and 60 mm/min with a speed of 1200 rpm. The highest hardness is achieved at 1200 rpm with the lowest feed rate of 20 mm/min. At 1600 rpm, ample heat is generated, but due to the low feed rate, heat dissipation occurs before the tool engages. When the feed rate is set at 40 mm/min, the sequence of maximum to minimum hardness is observed at 800, 1600, and 1200 rpm, respectively. In the cases of feed rates of 60 and 80 mm/min, the peak hardness consistently appears at 1600 rpm, while the lowest hardness is recorded for both speeds of 800 and 1200 rpm. FSP is used to eliminate the porosity in the interlayer, which is formed due to the additive manufacturing of 4043 aluminum alloy. After the FSP process, the mechanical properties and microstructure were observed and validated with the material without FSP. The average yield and ultimate were 88 and 148 MPa, respectively. The fatigue strength and elongation increased by 28% and 108.7%, respectively. The material after FSP will have high ductility and fatigue performance [28].

Generally, the hardness decreased below that of the base material in the thermo-mechanical and heat-affected zones. The increase in hardness seen in this experiment, due to strain hardening caused by magnesium presence, is crucial. However, it's noted that excessive brittleness can occur relative to the parent material. Thus, the selection of an appropriate tool speed and feed rate is critical for successful friction stir processing/welding, as lower material hardness than the base material may lead to weaker joints and reduced joint efficiency. Given that friction stir processing is a supplementary process, the resulting properties should surpass those of the initial material.

4.1 Wear Test

During the wear testing phase, the experiment involves the measurement of frictional forces, which are then recorded within the software. These measurements are taken at millisecond intervals and subsequently extracted in Excel format upon experiment completion. The resultant data are many more hence, the average coefficient of friction was computed every 15 seconds. This averaged data was employed for plotting in Figure 6, encompassing all combinations of process parameters. For comparative purposes, an investigation into the wear properties of the base material was also conducted under identical conditions to gauge any alterations brought about by processing. Key observations indicate that heightened hardness across all speeds leads to increased wear resistance and a reduction in friction coefficient, as indicated in Figure 6.

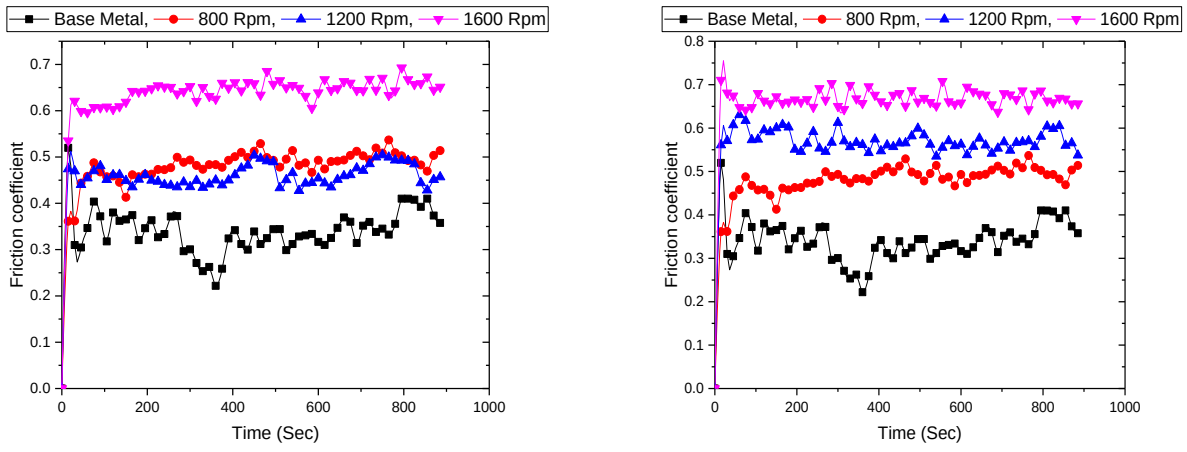

(a) (b)

Figure 6. Friction Coefficient versus time graphs, FSP specimen compared with base metal for different feed (a) 20 mm/min, (b) 40 mm/min;

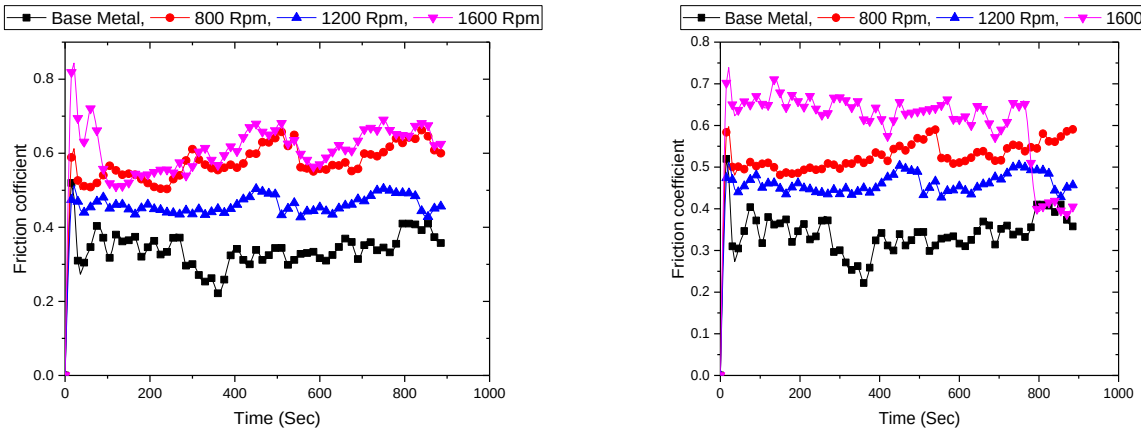

(c) (d)

Figure 6. (cont.) (c) 60 mm/min and (d) 80 mm/min

The increases in wear resistance are due to the incorporation of nanoparticles uniformly distributed within the AA5083 through friction stir processing involving either single or triple passes [4]. Additionally, the reinforcement of hard particles within the AA6061 series contributes to increased wear resistance compared to the original material [5]. Furthermore, the wear properties of the 6067-T6 hybrid composite, fabricated via friction stir processing, reveal that the silica particles bear load capacity while graphite acts as a solid lubricant, resulting in a low wear rate [6]. Notably, wear samples are selectively collected from the nugget zone due to its fine grain refinement.

Table 3. Average coefficient of friction for different speed and feed rate

Tool Speed (rpm)	Feed Rate (mm/min)			
	20	40	60	80
800	0.473	0.344	0.565	0.519
1200	0.457	0.575	0.511	0.398
1600	0.635	0.667	0.604	0.614

Wear resistance displays a direct correlation with hardness, a trend evident across all scenarios in the experiment. Consequently, friction coefficients also rise correspondingly. Among various speeds, the friction coefficient peaks at 1600 rpm across all feed rates, showcasing an increase of up to 48% compared to the parent material. At 1200 rpm, the increase ranges from 14% to 40% for feed rates of 80 mm/min and 40 mm/min, respectively. For the lowest speed of 800 rpm, the rise reaches 40% for a feed rate of 60 mm/min. If the speed and feed rate combination is low, material heat dissipation and hardening occur before the tool engagement. On the other end, higher combinations may lead to overly soft material due to excessive feed rates. The optimal feed rate seems to be 40 mm/min, as hardness and friction coefficient exhibit an inverse relationship with decreasing speed. Similarly, at a feed rate of 60 mm/min, 800 rpm and 1600 rpm display analogous behaviors due to variations in heat production and mechanical properties. In the case of an 80 mm/min feed rate, 800 rpm yields superior properties than 1200 rpm due to the tool's faster point engagement, although insufficient heat prevents base material softening.

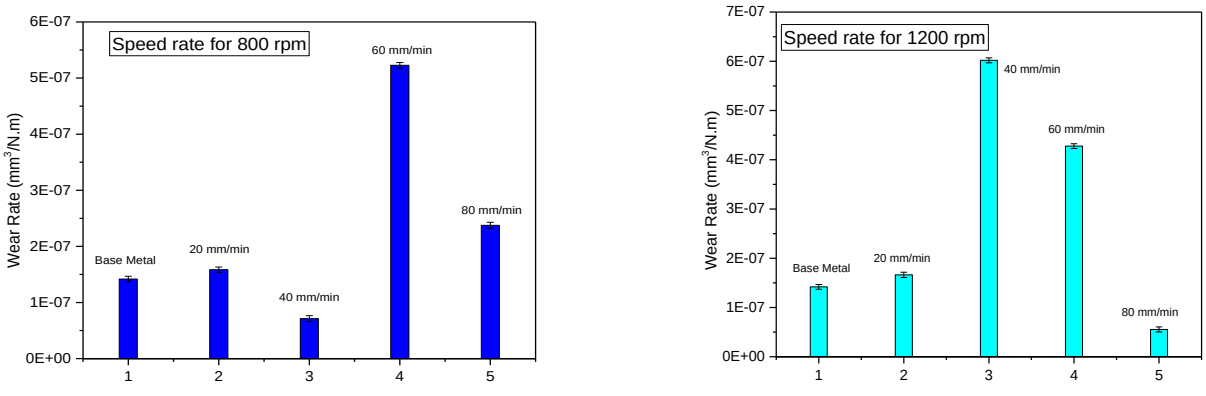

(a) (b)

Figure 7. Wear rate of base material compared with different feed rates (mm/min) for the different speeds (a) 800 rpm, (b) 1200 rpm

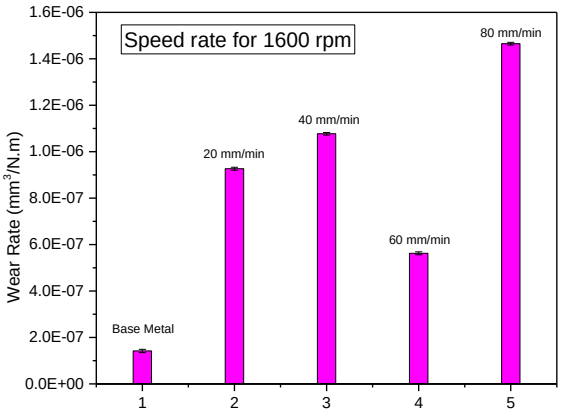

(c)

Figure 7. (cont.) (c) 1600 rpm

Wear rate analysis, shown in Figure 7, shows that processed surfaces are harder than the parent material, causing an increase in wear rate due to enhanced force resistance, ultimately leading to material degradation. Dissimilar aluminum composites, AA2024 and AA2014-based, were modified by using FSP, and the refinement of the secondary composite is uniform and enhances the wear properties. Hardness and tensile properties were increased due to the fine refinement of grains [31]. For the speed rates of 800 and 1200 rpm, the change in the wear rate is small and, in two cases, less than that of the parent material. Also, because the material may be softened or secondary alloys may not be even, in the last case, i.e., at 1600 rpm, the speed is enough to produce sufficient heat, but the feed rates will affect the wear properties because mechanical strain dominated over thermomechanical strains. Among the process parameters, tool speed and feed rate emerge as pivotal factors in enhancing mechanical properties. During the FSP processes, parameters such as speed varied from 800 to 1400 rpm, transversal speed ranged from 50 to 200 mm/min, and cooling mediums varied such as air, water-dry ice mixture, and liquid nitrogen. Mechanical and microstructure properties were studied and characterized. The grain refinement was down by less than 1 μm and activated the corrosion resistance phenomenon. The speed of 800 rpm and feed rate of 200 mm/min will have the highest corrosion resistance rate [27]. Average friction coefficients, presented in Table 3, illustrate that the highest average coefficient of friction occurs at 1600 rpm for all feed rates. Specifically, at a feed rate of 40 mm/min, the friction coefficient diminishes as speed decreases. However, for feed rates of 60 mm/min and 80 mm/min, the lowest coefficient of friction is seen at 1200 rpm and 800 rpm, respectively. Wear rate comparison reveals that specimens processed at 1600 rpm exhibit higher wear rates than those at 800 rpm and 1200 rpm. Yet, for a feed rate of 40 mm/min at 800 rpm and 80 mm/min at 1200 rpm, wear rates are lower than the base material. Nonetheless, other speed and feed rate combinations manifest increased wear rates in contrast to the base material. A consistent trend of escalating wear rates with increasing speed is observable for feed rates of 20 mm/min and 40 mm/min. Furthermore, for feed rates of 40 mm/min and 60 mm/min, wear rates are notably lower at 1200 rpm when compared to the other speeds of 800 rpm and 1600 rpm.

4.2 Microstructure

The investigation into the microhardness results led to a thorough examination of the worn surfaces after the wear test. Scanning electron microscopy (SEM) was employed to scrutinize the worn surfaces, and the corresponding images can be found in Figures 8-11. These images, captured consistently at an intensity over a 40 μm span, revealed notable insights. Specifically, the secondary alloy magnesium exhibited an uneven distribution, accumulating predominantly near the surface of the parent material. Notably, during the wear process, the hardened magnesium was found to induce heightened wear, counterbalanced by the lubricating properties of the aluminum, which acted as a solid lubricant, thereby mitigating wear.

The SEM images, especially those in Figure 8 (a) and (b), displayed uniform grooving with shallow depths. Additionally, the images displayed particle plugging and the presence of thin debris. Shifting the focus to Figure 9 (a), (b), (c), and (d), showcasing worn surfaces from the wear test at 800 rpm rotational speed and varying feed rates, the intricate interplay of speed and feed rate on material properties became apparent. Notably, lower speeds and reduced feed rates led to heightened heat dissipation, resulting in scratched and deeply grooved wear surfaces. Interestingly, a feed rate of 60 mm/min demonstrated a smooth sliding wear pattern, yielding an evenly worn surface compared to other feed rates. In stark contrast, feed rates of 20 mm/min and 40 mm/min led to the development of a brittle surface with deep grooves and an increased prevalence of cracks. Even at a feed rate of 80 mm/min, any observed variations in properties were attributable to the feed rate, rather than the rotational speed. Sliding behavior remained uniform, albeit with minor cracks. A Magnesium alloy-based hybrid composite was fabricated using multi-pass friction stir processing (FSP) to enhance its mechanical properties. The grain size was reduced from 63 to 3.5 μm. The percentage elongation of the double pass

fabricated composite was found to be 32.7%, marking an enhancement of 83% in ductility as compared to the base metal [32].

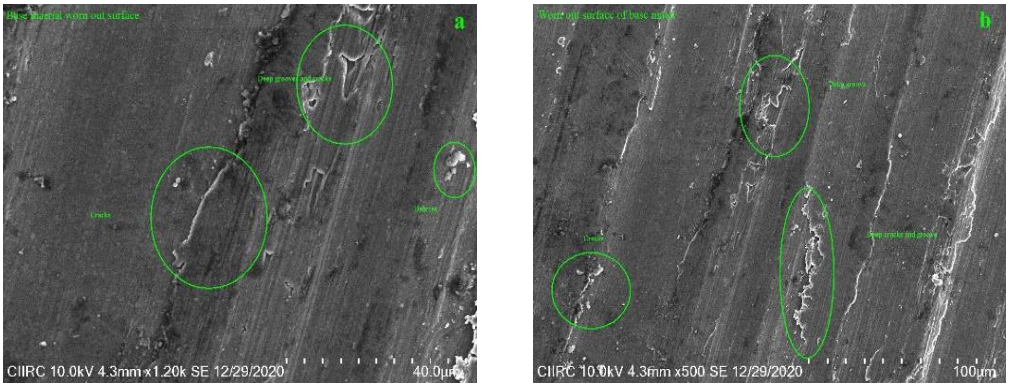

(a) (b)

Figure 8. Scanning electron microscope image of the worn surface of samples, (a) base metal at 40µm (b) base metal at 100µm

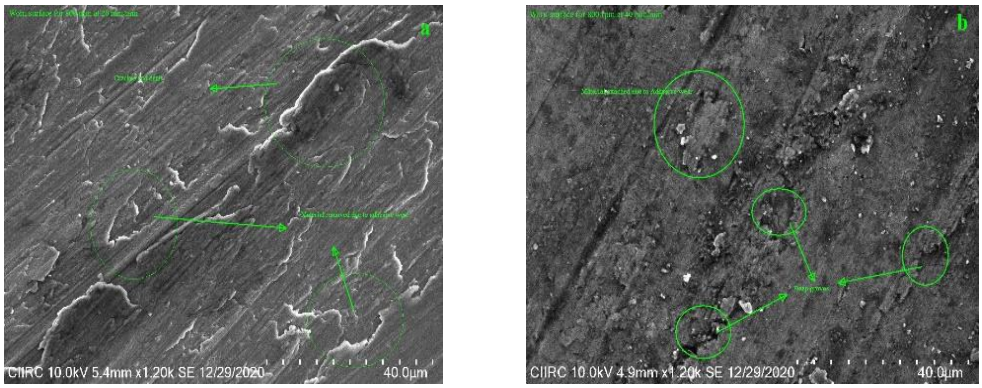

(a) (b)

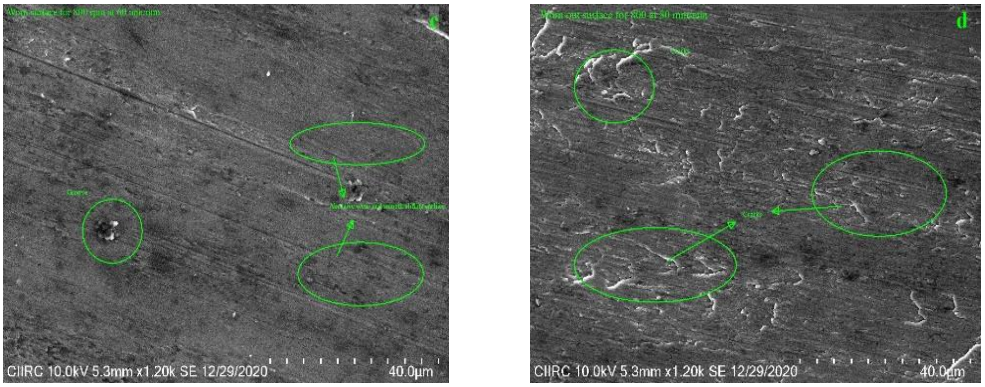

(c) (d)

Figure 9. Scanning electron microscope image of the worn surface at 800 rpm, feed rate of (a) 20 mm/min, (b) 40 mm/min, (c) 60 mm/min and (d) 80 mm/min

In the second trial involving a rotational speed of 1200 rpm, the heat generated due to friction surpassed that of the 800 rpm setting. Consequently, the material underwent softening, yielding a uniformly worn surface. This was especially evident in the SEM images found in Figure 10 (a), (b), (c), and (d), which pertained to feed rates of 20, 40, 60, and 80 mm/min, respectively. Notably, only at the feed rate of 80 mm/min did some cracks and rough surfaces emerge, likely due to inadequate heat generation for material softening. A distinct trend emerged upon comparing the 1200 rpm worn surface to the smoother nature of the 800-rpm worn surface, a phenomenon attributed to the material's softening with increased speed. The fatigue and fretting fatigue of AA6063 alloys after FSP were studied. The ultimate tensile strength, fatigue, and fretting fatigue increased by 31.6%, 10%, and 28.3%, respectively. The fretting wear damage and coefficient of friction were higher in the FSP surface compared with the base material. The fatigue life was reduced by 1.6 and 1.18 times [33].

(a)

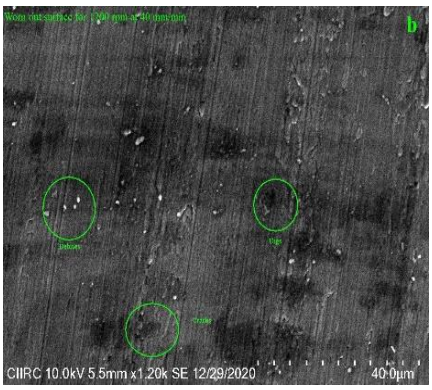

(b)

(c)

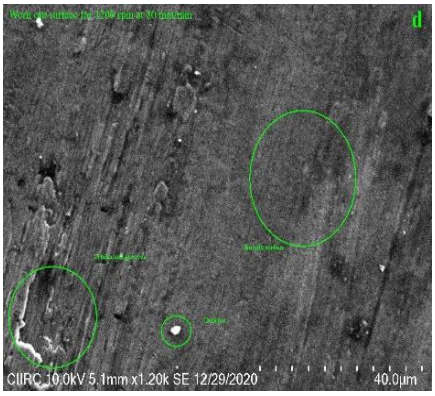

(d)

Figure 10. Scanning electron microscope image of worn surface at 1200 rpm, feed rate of (a) 20 mm/min, (b) 40 mm/min, (c) 60 mm/min, and (d) 80 mm/min

(a)

(b)

(c)

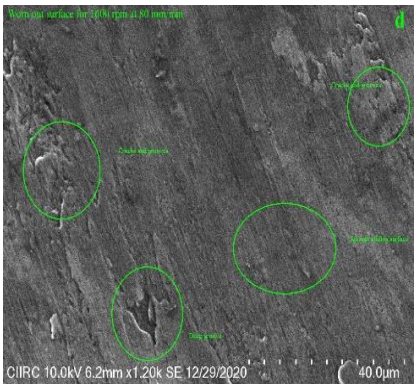

(d)

Figure 11. Scanning electron microscope image of worn surface at 1600 rpm, feed rate of (a) 20 mm/min, (b) 40 mm/min, (c) 60 mm/min, and (d) 80 mm/min

Lastly, the examination of the worn surface following wear testing at a rotational speed of 1600 rpm yielded intriguing results. In comparison to the two lower speeds, a more uniformly sliding surface was observed, characterized by a scarcity of deep grooves and cracks. Notably, subtle grooves were discernible on the surface, potentially arising from hardened particles adhering to the disk during wear testing, thereby initiating localized wear. The feed rate of 80 mm/min exhibited a limited number of dents and cracks, indicative of insufficient heat to soften the material at this specific feed rate.

5.0 CONCLUSION

The investigation into the tribological and hardness properties of AA-2Mg alloys post-friction stir processing explores the effects of varied process parameters. It was observed that the most notable enhancement in hardness, a remarkable 26% increase, occurred at a rotational speed of 1600 rpm coupled with a feed rate of 60 mm/min, showcasing a substantial improvement over the base metal. Furthermore, the average frictional coefficient exhibited a discernible escalation, particularly evident at the 1600 rpm speed across all feed rate combinations, suggesting a consistent trend of increased frictional behavior at higher rotational speeds. Moreover, significant increments in frictional coefficient percentages were noted across different feed rates: 46% for 20 mm/min, 49% for 40 mm/min, 44% for 60 mm/min, and 45% for 80 mm/min, all in comparison to the parent material. These findings underscore the intricate interplay between process parameters, hardness, and frictional behavior in AA-2Mg alloys subjected to friction stir processing, offering valuable insights for optimizing the process to achieve desired material properties.

6.0 REFERENCES

[1] W.M. Thomas, E.D. Nicholas, J.C. Needham, M.G. Murch, P.T. Smith, and C.J. Dawes. G. B, Patent No. 9125978.8, Dec 1991.

[2] R.S. Mishra, and Z.Y. Ma, "Friction stir welding and processing," *Materials Science & Engineering*, vol. 50, pp. 1-78, 2005.

[3] R.S. Mishra, Z.Y. Ma, and I. Charit, "Friction stir processing: a novel technique for fabrication of surface composite," *Materials Science and Engineering*, vol. 341, no. 1-2, pp. 307-310, 2003.

[4] S. Kumar, A. Divakaran, and S.V. Kailas, "Fabrication and tribo characteristics of in-situ polymer dervied nano ceramic composites of Al-Mg-Si alloys," *Tribology International*, vol. 180, pp. 108272, 2023.

[5] S. Nabi, S. Rathee, and M. Srivastava, "Friction and Wear analysis of Al-5052/NiTi surface composites fabricated via friction stir processing," *Tribology International*, vol. 191, p. 109179, 2024.

[6] Poovazhangan, Lakshmanan, G.R. Ravanneswarran, S. Sanjai and G. Kumanan, "Examining the abrasive wear properties of LM22 aluminum alloys reinforced with SiC and B4C nanoparticles," *Materials Today Proceedings*, vol. 62, no. 2, pp. 589-597, 2022.

[7] A. Adetunla, and E.T. Akinabi, "Investigating the effects of process parameters on the mechanical integrity of friction stir processed aluminium alloys," *Materials todays proceedings*, vol. 44, no. 1, pp. 1238-1242, 2021.

[8] H. Nayak, N. Krishnamurthy and R.A. Shailesh, "Development and adhesion strength of plasma-sprayed thermal barrier coating on the cast iron substrate," *International Journal of Integrated Engineering*, vol. 13, no. 1, pp. 47-59, 2021.

[9] B. Shaik, G.H. Gowd, and B.D. Prasad, "Experimental and parametric studies with friction stir welding on aluminium alloys," *Materials Today Proceedings*, vol. 19, no. 2, pp. 372-379, 2019.

[10] D. Ahmadkhaniha, M.H. Sohi, A. Zarei-Hanzaki, S.M. Bayazid, and M. Saba, "Taguchi optimization of process parameters in friction stir processing of pure Mg," *Journal of Magnesium and Alloys*, vol. 3, no. 2, pp. 168-172, 2015.

[11] J. Li, F. Cao, and Y. Shen, "Effect of welding parameters on friction stir welded Ti-6Al-4V joins: Temperature, Microstructure and Mechanical properties," *Metals*, vol. 10, no. 7, pp. 940, 2020.

[12] K. Fuse, and V. Badheka, "Effect of shoulder diameter on bobbin tool friction stir welding of AA 6061-T6 alloys," *Materials Today Proceedings*, vol. 42, no. 2, pp. 810-815, 2021.

[13] J.S. Leon, G. Bharathiraja, and V. Jayakumar, "Durability map of the friction stir welding tools with flat faced pins," *International Journal of Integrated Engineering*, vol. 12, no. 8, pp. 83-96, 2020.

[14] D.B. Darmadri, A. Mentary, E.M. Yusup and S. Mahzan, "Evaluating the effect of the pin's length to the strength of double slides Friction stir welded aluminium," *International Journal of Integrated Engineering*, vol. 11, no. 5, pp. 1-11, 2019.

[15] R.M. Vaidyanathan, N. Sivaraman, M. Patel, M.M. Woldegioris, and T.A. Atiso, "A revies on the effect of shoulder diameter to pin diameter (D/d) ratio on friction stir welded aluminium alloys," *Materials Today Proceedings*, vol. 45, no. 6, pp. 4792-4798, 2021.

[16] The Aluminium Association, Inc. 1998. Selection and application., http://calm-aluminium.com.au/Documents/Aluminium-Alloys.pdf

[17] ASTM International, 2022. "Standard Test Method for Microindentation Hardness of materials (E384-22). ASTM International.

[18] ASTM International, 2017. "Standard Test Method for Wear Testing with a Pin-on-Disk Apparatus, (G99-17). ASTM International.

[19] S. Bharti, V. Dutta, S. Sharma, and R. Kumar, "A study on the effect of friction stir processing on the hardness of aluminium 6000 series," *Material today proceedings*, vol. 18, pp. 5185-5188, 2019.

[20] P. Jeyapandiarajan, J. Joel, P. Pramesh, N. Dugar, S. Chandok, and M.A. Xavior, "Evaluating the mechanical characteristics of aluminium alloy 2285 processed by friction stir processing," *Materials Research Express*, vol. 6, no. 1, p. 016528, 2018.

[21] A. Samanta, R.J Seffens, H. Das, A.D. Guzman, T.J. Roosendaal, D. Garcia, et al., "Microstructure-refinement-driven enhanced tensile properties of high pressure die casting A380 alloys through friction stir processing," *Journal of Manufacturing Processes*, vol. 78, pp. 352-362, 2022.

[22] S. Ahmed, R.A. ur Rahman, A. Awan, S. Ahmad, W. Akram, M. Amjad, et al., "Optimization of Process Parameters in Friction Stir Welding of Aluminum 5451 in Marine Applications," *Journal of Marine Science and Engineering*, vol. 10, no. 10, pp. 1539, 2022.

[23] E.B. Moustafa, M.A. Alazwari, W.S. Abushanab, E.I. Ghandourah, A.O. Mosleh, H.M. Ahmed, et al, "Influence of friction stir process on the physical, microstructural, corrosive, and electrical properties of an Al–Mg alloy modified with Ti–B Additives," *Materials (Basel)*, vol. 15, no. 3, pp. 835 , 2022.

[24] K.V. Mjali, and Z.A. Mkoko, "Varying rotational speeds and their effect on the mechanical properties of friction stir welded 6082-T651 aluminium alloy plates," *Manufacturing Letters*, vol. 35, pp. 305-313, 2022.

[25] V. Feizollahi, and A.H. Moghadam, "Effect of pin geometry, rotational speed, and dwell time of tool in dissimilar joints of low-carbon galvanized steel and aluminum 6061-T6 by friction stir spot welding," *Materials*, vol. 20, pp. 100-483, 2023.

[26] Gh. Asrari, M.H. Daneshifar, S.A. Hosseini, and M. Alishahi, "Selective alloying of pure aluminum with varying amounts of magnesium using friction stir processing for improved mechanical and corrosion-resistant properties," *Materials Chemistry and Physics*, vol. 306, p. 128091, 2023.

[27] S.S. Mirian Mehrian, M. Rahsepar, F. Khodabakhshi, and A.P. Gerlich, "Effects of friction stir processing on the microstructure, mechanical and corrosion behaviors of an aluminum-magnesium alloy," *Surface and Coatings Technology*, vol. 405, p. 126647, 2021.

[28] C. He, J. Wei, Y. Li, Z. Zhang, N. Tian, G. Qin, et al., "Improvement of microstructure and fatigue performance of wire-arc additive manufactured 4043 aluminum alloy assisted by interlayer friction stir processing," *Journal of Materials Science and Technology*, vol. 133, pp. 183-194, 2023.

[29] A. Baghdadchi, V. Patel, W. Li, X. Yang and J. Andersson, "Ductilization and grain refinement of AA7075-T651 alloy via stationary shoulder friction stir processing," *Journal of Materials Research and Technology*, vol. 27, pp. 5360-5367, 2023.

[30] G. Yang, W.Q. Zhang, J. Zhang, J.Z. Yi and Y.F. Cui, "Evolution of microstructure of WE43 magnesium alloys fabricated by laser deposition manufacturing with subsequent friction stir processing," *Materials Letters*, vol. 330, pp. 133-218, 2023.

[31] S.P. Dwivedi, S. Sharma, C. Li, Y. Zhang, A. Kumar, R. Singh, et al., "Effect of nano-TiO2 particles addition on dissimilar AA2024 and AA2014 based composite developed by friction stir process technique," *Journal of Materials Research and Technology*, vol. 26, pp. 1872-1881, 2023.

[32] A. Maqbool, and N. ZamanKhan, "Fabrication and characterization of hybrid WE43 Mg alloy-based composite by friction stir processing with improved ductility," *Vacuum*, vol. 215, pp. 112-273, 2023.

[33] M. Patel, S. Sangral, J. Murugesan and Y. Mutoh, "Effect of friction stir processing on plain fatigue and fretting fatigue behaviour of the AA6063 alloys," *Tribology International*, vol. 186, pp. 108-642, 2023.